Human Molecular Genetics, 1997, Vol. 6, No. 7 **1079–1086**

Translocation breakpoint maps 5 kb 3′ from *TWIST* in a patient affected with Saethre–Chotzen syndrome

Inge Krebs[1], Isabel Weis[1], Melanie Hudler[1], Johanna M. Rommens[2], Helmut Roth[1], Steven W. Scherer[2], Lap-Chee Tsui[2], Ernst-Martin Füchtbauer[3], Karl-Heinz Grzeschik[1], Kazushiro Tsuji[4] and Jürgen Kunz[1,*]

[1]Philipps-Universität Marburg, Medizinisches Zentrum für Humangenetik, Bahnhofstrasse 7, D-35033 Marburg, Germany, [2]Hospital for Sick Children, Department of Genetics, 555 University Avenue, Toronto, Ontario M5G 1X8, Canada, [3]Max-Planck Institut für Immunbiologie, Stübeweg 51, D-79108 Freiburg, Germany and [4]Okoyama University Medical School, Department of Pediatrics, Okoyama, Japan

Received February 3, 1997; Revised and Accepted April 9, 1997 DDBJ/EMBL/GenBank accession nos Y11177-Y11180

Saethre–Chotzen syndrome, a common autosomal dominant craniosynostosis in humans, is characterized by brachydactyly, soft tissue syndactyly and facial dysmorphism including ptosis, facial asymmetry, and prominent ear crura. Previously, we identified a yeast artificial chromosome that encompassed the breakpoint of an apparently balanced t(6;7) (q16.2;p15.3) translocation associated with a mild form of Saethre–Chotzen syndrome. We now describe, at the DNA sequence level, the region on chromosome 7 affected by this translocation event. The rearrangement occurred ~5 kb 3′ of the human *TWIST* locus and deleted 518 bp of chromosome 7. The *TWIST* gene codes for a transcription factor containing a basic helix–loop–helix (b-HLH) motif and has recently been described as a candidate gene for Saethre–Chotzen syndrome, based on the detection of mutations within the coding region. Potential exon sequences flanking the chromosome 7 translocation breakpoint did not hit known genes in database searches. The chromosome rearrangement downstream of *TWIST* is compatible with the notion that this is a Saethre–Chotzen syndrome gene and implies loss of function of one allele by a positional effect as a possible mechanism of mutation to evoke the syndrome.

INTRODUCTION

Craniosynostosis (CRS), the premature fusion of one or more cranial sutures, is a relatively common developmental anomaly that causes an abnormal shape of the skull (1). Many of those affected require major craniofacial surgery. The frequency of CRS has been estimated to be in the order of 1 in 3000 infants (2). CRS may occur as an isolated anomaly or in association with other congenital anomalies as part of the various craniosynostosis syndromes. More than 100 different forms of isolated craniosynostosis and craniosynostosis syndromes are known, showing etiologic and pathogenetic heterogeneity (3). In about half of the syndromes, a genetic cause has been established or suggested. Most syndromes with a genetic background are inherited as monogenic autosomal dominant traits (4).

The acrocephalosyndactylies (ACS) comprise a clinically similar group among the autosomal dominant craniosynostosis syndromes, characterized by coronal or multiple synostoses in association with distal limb anomalies, in particular syndactyly (3). Blank (5) proposed a classification into a typical and an atypical form. The typical form is Apert syndrome, characterized by syndactyly of hands and feet of a special type (complete distal fusion with tendency for fusion also of the bony structures). The second group, atypical non-Apert ACS, was thought to comprise a heterogeneous collection of disorders and includes Crouzon, Jackson–Weiss, Pfeiffer, and Saethre–Chotzen syndromes. The overlap in phenotype of the ACS syndromes complicates diagnosis, and there has been extensive discussion about which syndromes should be regarded as separate entities. Recently, the genetics of several ACS syndromes was resolved, and a new classification system based on genotype is being established.

Wilkie and co-workers (6) identified specific missense substitutions of fibroblast growth factor receptor 2 (*FGFR2*) involving adjacent amino acids in the linker between the second (Ig II) and third (Ig III) immunoglobulin-like domain in all 40 unrelated cases of Apert syndrome they studied. Allelic mutations in the main part of Ig III domain of *FGFR2* have been identified in Pfeiffer and Jackson–Weiss craniosynostosis syndromes (7–10) and in Crouzon syndrome (7,11–16). Whereas these latter CRS syndromes result from a variety of different *FGFR2* point mutations, with in some cases, identical mutations giving rise to more than one syndrome, the mutations responsible for Apert syndrome are very specific (17).

Saethre–Chotzen syndrome (ACS, MIM 101400) shares features with other ACS syndromes such as coronal suture synostosis, but in addition facial asymmetry, high incidence of ptosis, deviated nasal septum, low frontal hairline, brachydactyly, partial cutaneous syndactyly and small ears with prominent crura are observed (18,19). The frequency of this condition is ~1 in 25 000 to 1 in 50 000 live births, and this may be underestimated (20). Saethre–Chotzen syndrome segregates as an autosomal

*To whom correspondence should be addressed. Tel: +49 6421 283576; Fax: +49 6421 288920; Email: kunzj@mailer.uni-marburg.de

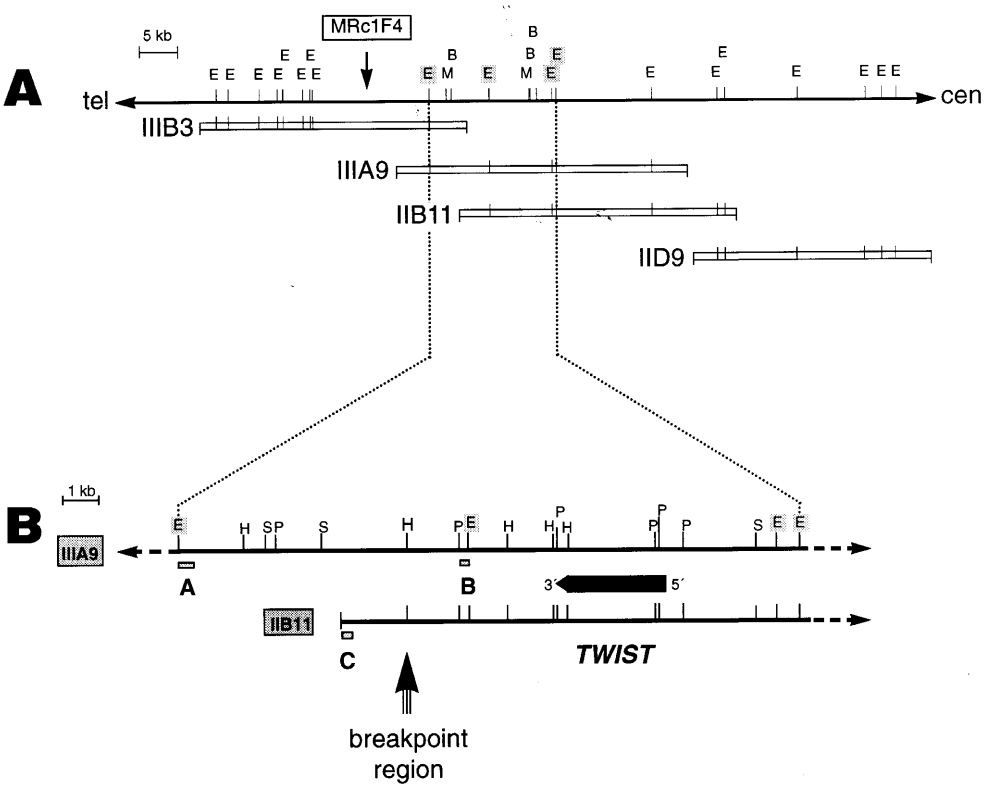

Figure 1. Physical mapping of the TWIST region. (**A**) Restriction map of the cosmid contig interval between clones IIIB3 and IID9 which were identified by FISH to flank the translocation breakpoint. tel, towards telomere; cen, towards centromere; E, *Eco*RI; M, *Mlu*I; B, *Bss*HII. The localization of the cDNA clone MRc1F4 is indicated by an arrow. (**B**) Refined physical map of a 16.7 kb interval containing the breakpoint. E, *Eco*RI; H, *Hin*dIII; P, *Pst*I; S, *Sac*I. The position of the fragments used as probes A–C to close in the breakpoint is indicated. Probes A and C hybridize to the telomeric side of the breakpoint, probe B to the centromeric side. From the sequences of probes A, B and C, primers were selected to define STSs MR23006, MR23007 and MR22002 (Table 1). The positions of the breakpoint region and the *TWIST* region resulting from sequence analysis (accession nos. X91662 and X99268) (Fig. 3) are indicated.

dominant trait and shows variable phenotype. This variable expression of the disease leads to problems in diagnosis. The location of the responsible gene has recently been mapped to chromosome 7p (21). Subsequently, cytogenetic and linkage analyses have enabled the physical interval encompassing the disease gene to be delimited to a short region of chromosome, 7p15.3–p21.2 (22–26). Most recent findings identified mutations in the gene of a basic helix–loop–helix transcription factor, *TWIST*, localized on chromosome 7p21–p22, causing this disease (20,27).

We previously described a sporadic case of Saethre–Chotzen syndrome with a t(6;7)(q16.2;p15.3) translocation and identified a YAC clone spanning the breakpoint (28). Now we present a detailed physical and transcription map of the breakpoint region and show that the translocation event splits chromosome 7 about 5 kb downstream of *TWIST* deleting 518 bp from this region. Potentially, in this case the syndrome is caused by a positional effect on *TWIST* expression.

RESULTS

Cosmid contig spanning a translocation breakpoint region associated with Saethre–Chotzen syndrome

YAC clone 933_e_1 from the Centre d'Etudes du Polymorphisme Humaine (CEPH) which we had previously shown by fluorescence *in situ* hybridization (FISH) to span the breakpoint on chromosome 7 in a craniosynostosis patient with an apparently balanced translocation t(6;7)(q16.2;15.3) (28) was subcloned and ordered into a contiguous array of cosmid clones. 254 cosmids containing human inserts representing a 9-fold coverage of the YAC insert DNA were arranged by *Alu*-PCR fingerprinting, *Eco*RI fingerprinting, and hybridization of arrayed clones on filters with selected cosmid inserts and with YAC insert end fragments. The whole length of the YAC is represented in a minimum tiling path of 32 clones (data not shown). FISH of DNA from individual cosmid clones to metaphase chromosomes of the translocation patient identified clones IIIB3 and IID9 flanking the chromosome breakpoint at the telomeric and centromeric side, respectively (Fig. 1A). These cosmids are connected by clones IIIA9 and IIB11 which appear to span the translocation breakpoint. These four clones were chosen to define the breakpoint at the sequence level and to identify genes close by.

Mapping and sequencing across the translocation breakpoint

About 100 kb covered by cosmid clones IIIB3 to IID9 were subjected to detailed restriction mapping (Fig. 1A). STS probes A and B (Fig. 1B; see also Table 1) were generated by sequencing the ends of an 8.0 kb *Eco*RI fragment. In Southern blots with DNA from the patient probe A detected the original 8.0 kb *Eco*RI and an additional band of ~12.0 kb which is thought to represent the derivative chromosome 7 telomeric site translocated onto the $6q^-$ chromosome (Fig. 2A). Probe B identified in addition to the

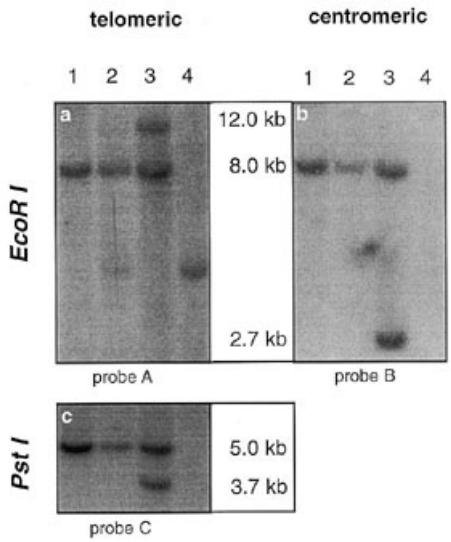

Figure 2. Altered restriction fragment sizes due to the t(6;7) translocation. Genomic DNA from human control , 46,XX (GM3104) (1); chromosome 7 monochromosomal cell hybrid (5387-3cl10) (2), t(6;7)(q16.2;p15.3) translocation patient cell line (3), and mouse control cell line (Rag) (4) were digested with the restriction enzyme indicated. Southern blots were hybridized with probes from the telomeric (**A** and **C**) and centromeric side (**B**) of the breakpoint region on chromosome 7. In the patient's DNA (lane 3), besides the bands present in the controls, additional fragments are detected which represent the $6q^-$ and $7p^+$ translocation chromosomes. Primer pairs for generating probes A, B and C are listed in Table 1.

normal band a smaller 2.7 kb *Eco*RI fragment which should be the chromosome 7 centromeric part of the translocation product remaining on the derivative chromosome $7p^+$ (Fig. 2B). To narrow down the breakpoint from the telomeric side, genomic DNA from the patient was digested with *Pst*I. Hybridization with probe C, derived from the telomeric end of cosmid IIB11, detected instead of the expected 5.0 kb an aberrant 3.7 kb *Pst*I fragment, representing the telomeric side of the translocation event (Fig. 2C).

By cloning and partial sequencing of the rearranged 2.7 kb *Eco*RI and the 3.7 kb *Pst*I fragment and comparison with the sequence of the original 8.0 kb *Eco*RI fragment encompassing the breakpoint revealed that chromosome 7 was broken and that a segment of 518 bp between the breakpoints was deleted (Fig. 3). This deletion had occurred *de novo* since in PCR analysis using the primer pair MR22008/MR22010 (Table 1), genomic DNA of the patient's parents did not reveal an altered product length indicative of a deletion (data not shown). Database analysis of the chromosome 6 derived sequences from the breakpoints indicated that on the der(7) side of the translocation a human specific *Alu* element was detected beginning within position 260 and extending into a 3′ poly A stretch (Fig. 3; accession no. X54175).

cDNA selection

To detect (a) candidate gene(s) causing craniosynostosis and/or Saethre–Chotzen syndrome in the breakpoint region we employed both a cDNA selection strategy and genomic sequence analysis. cDNA selection from an array of different cDNA libraries was performed with pooled DNA cosmids IIIB3 to IID9. Seventy of the selected cDNA clones (~18% of the clones) appeared to be non-repetitive and were analyzed in more detail. Sequencing of cDNA clones showed that of the five clones mapping back to the original cosmids, two MRc2A2 (accession no. Y11177) and MRc1F5 (635 bp) were identical and three other clones were unique [cDNA MRc1F4 (277 bp) (accession no. Y11180), MRc10D6 (339 bp) (accession no. Y11178), and MRc7F11(406 bp) (accession no. Y11179)]. cDNA clones MRc2A2, MRc1F5, MRc10D6 and MRc7F11 mapped to an 8.1 kb *Eco*RI fragment of the cosmids IIIA9 and IIB11 adjacent to the 8.0 kb *Eco*RI fragment affected by the translocation (Fig. 4). Homology searches of MRc2A2 and MRc1F5 indicated 98.2% similarity over a length of 393 bp to the UTR 3′ end of human cDNA sequence (position 1042–1435) of the gene *TWIST* (accession no. X99268). MRc2A2 extended the published sequence by 242 bp. Clone MRc10D6 reached from the 3′ end of the human *TWIST* gene over the intron–exon boundaries of exons 1 and 2 (Fig. 3A). The fourth clone MRc7F11 overlapped with the previous clones, resulting in a complete representation of exon 2 with parts of exon 1. The localization of *TWIST* in this region was confirmed by hybridization of an 800 bp *Eco*RI/*Xba*I fragment of a mouse cDNA clone (pT7T3 19U twist 1282) from *Twist* containing the coding region of the gene to restriction fragments of the cosmid contig. On Southern blots of *Eco*RI digested genomic DNA from the patient and controls hybridized with a selected *TWIST* UTR 3′-end cDNA clone (MRc2A2) no other fragment than the 8.1 kb *Eco*RI band was recognized. Thus the translocation does not affect the genomic structure of the *TWIST* gene region. Clone MRc1F4 is localized on the 12.0 kb *Eco*RI fragment of cosmid clone IIIB3 (Fig. 1A). Database searches for this EST clone did not detect homology to known sequences.

Screening for mutations in the coding region of *TWIST*

To exclude the possibility that the phenotype of the patient is caused by second-site mutations in *TWIST*, the entire coding region of *TWIST* was examined by sequencing two PCR products spanning the exon 1 region. Analysis of these sequences showed no difference from the published sequence (accession no. U80998).

Table 1. Oligonucleotide primers used to generate probes for detection of the translocation breakpoint region and for deletion analysis

Primer	Forward	Reverse	Ann. temp.	Product/bp	Probe
MR22002 f/r	5′-TCCAGGGTCGAGATTATTC	5′-AGACCCTAACAAATGTGGC	55°C	383	C
MR23006 f/r	5′-AAATAACGGTCTCAGGGC	5′-AGCTGAACAAGGATTCCC	55°C	358	A
MR23007 f/r	5′-GGAGCAGGTTAAAATCACTG	5′-CACGTAAACAAGAAAGGAGG	55°C	250	B
MR22010/MR22008	5′-ATTATGCCTGTAGGAAGCC	5′-CCACTTCCCACATTGCTCTC	55°C	760	STS

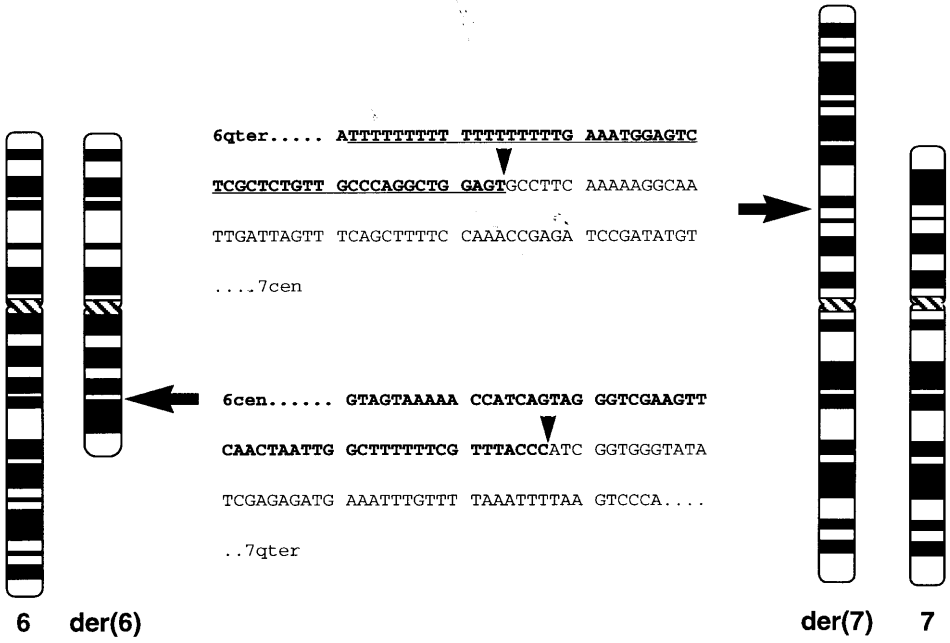

Figure 3. Sequence analysis of the t(6;7) translocation breakpoints. Sequences of the chromosome 6;7 junctions on the der(6) and der(7) chromosomes. Bold letters indicate the sequences derived from the chromosome 6 side of the translocation breakpoints on the der(6) and der(7) chromosome, respectively. The deleted chromosome 7 contains the basepairs 6009–6526 in the sequence with accession no. Y10871. Database analysis detected a high homology with a human specific*Alu* element (accession no. X54175) on the der(7) chromsome, derived from the chromosome 6 translocation partner (underlined).

Genomic sequence analysis

To complement the cDNA selection results, in total 14.5 kb genomic DNA encompassing the 8.0 kb *Eco*RI breakpoint fragment and the neighbouring 8.1 and 0.6 kb *Eco*RI fragments were sequenced and analysed walking from the ends of the *TWIST* sequence (accession no. X91662) (Fig. 4).

The single-base composition of the 16.7 kb sequence is A = 27.0%, T = 26.6%, C = 23.0% and G = 22.9% (accession no. Y10871). The weakbase bias (54.1% A+T versus 45.9% G+C) is typical for the human genomic sequence (29). Interestingly, with the exception of a new $(CA)_n$ dinucleotide repeat, no repetitive element, neither an *Alu* nor a LINE1 sequence was detected in this genomic region. The genomic sequence was analyzed using the software GRAIL 1+2, which detects potential exon structures, Basepairplot and BLASTX. Besides *TWIST* no further known genes were found in databases. However, several CpG islands and putative exons were detected in this segment (Fig. 4B and C). One CpG island could be identified which shows 95% similarity with two database entries (accession nos Z55345 and Z55346) (Fig. 4A).

DISCUSSION

This report describes the successive stages of the mapping and DNA sequencing of a translocation breakpoint at chromosome 7p15.3 associated with Saethre–Chotzen syndrome (26). Our results provide new information regarding the physical map of this region, the gene content near the translocation breakpoint and the DNA sequence of the human *TWIST* gene which has recently been shown to cause the disease (20,27). In our study we have determined that the translocation in this patient is associated with a *de novo* deletion of 518 bp and that the breakpoint resides ~5 kb (telomeric) on the 3′ site of the *TWIST* gene. Examination of the coding region of TWIST showed that the gene in this patient is not affected by any of the mutations described previously (20,27). Therefore, the short distance separating the chromosome breakpoint from *TWIST* suggests that it is the critical gene that causes the disease in this patient, as has been observed in familial cases (20,27).

TWIST codes for a nuclear DNA-binding protein containing a basic helix–loop–helix (b-HLH) motif suggesting it most likely functions as a transcription factor. The gene was first characterized in *Drosophila* as one of the zygotic genes required for dorsoventral patterning during embryogenesis. Interestingly, in mouse knockout experiments, Twist null (–/–) embryos exhibit failure of neural closure and die at day 11.5 p.c. (30). Mice heterozygous for the mutation (Twist +/–) showed a moderate phenotype including minor skull and limb anomalies (27). The isolation of *TWIST* from a variety of other species (*Xenopus*, mouse, human) showed that the protein is highly conserved. This is particularly true for the DNA binding domain and the helix–loop–helix region of the gene, both regions showed an absolute identity in all species. Interestingly, all mutations which were detected in Saethre–Chotzen patients affect these conserved regions, especially the DNA binding domain, the helix I and the loop structure (20,27).

Since no mutations in the coding region of the gene were observed and no other known gene(s) have been identified from the breakpoint region it is likely that the translocation event causes a position effect, perhaps by altering chromatin structure (31) or by separating *cis*-acting regulative regions from the gene.

The position effect phenomenon is likely to abolish or reduce the level of transcription of one copy of the gene resulting in haploinsufficiency or reduced protein levels at critical stages

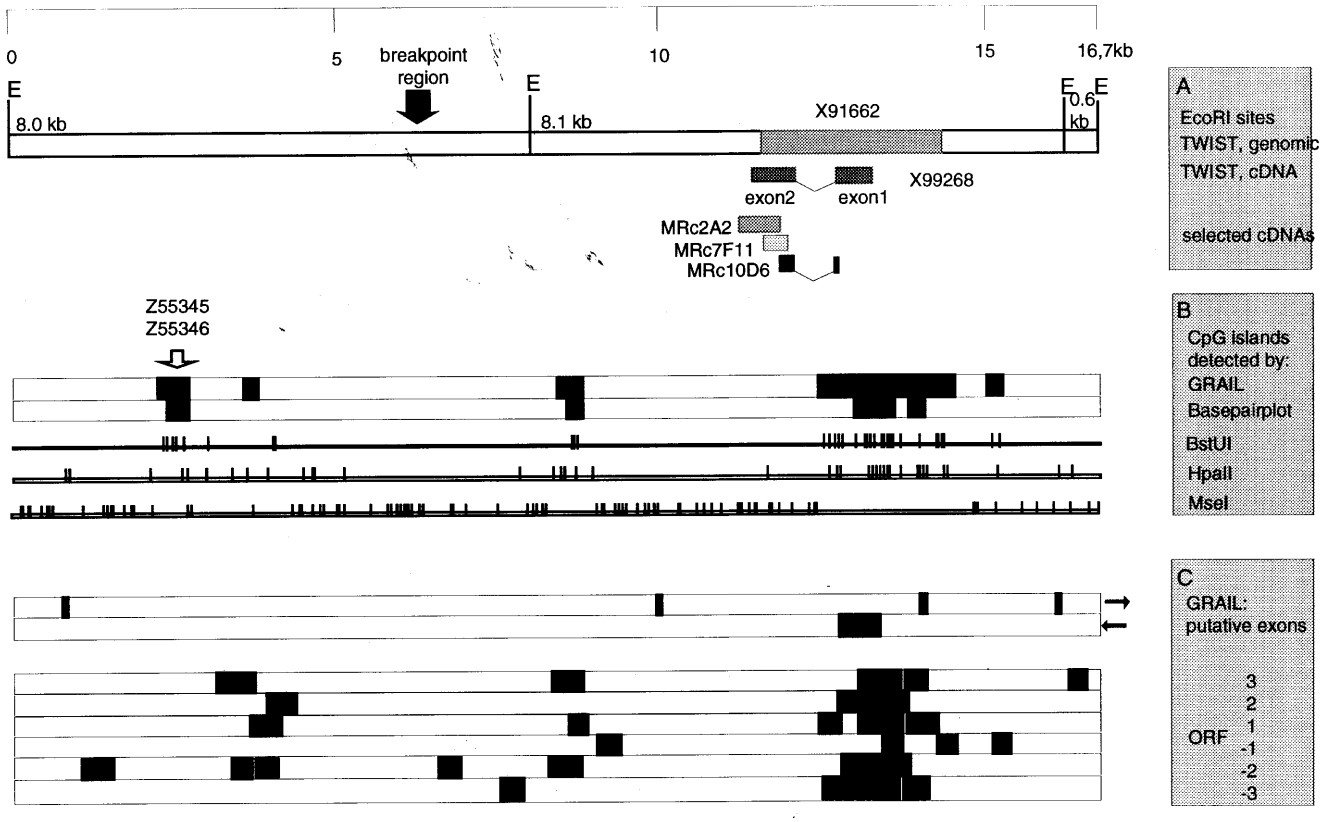

Figure 4. Search for transcribed sequences around the translocation breakpoint. (**A**) 14.5 kb from adjacent *Eco*RI fragments were sequenced (accession no. Y10871). The sequencing was directed from the published genomic *TWIST* sequence (shadowed grey; accession no. X91662) towards the ends of the restriction fragments (16.7 kb in total). The position of the t(6;7) translocation in the 8.0 kb *Eco*RI fragment is indicated by an arrow. cDNA selection found only fragments of *TWIST* cDNA within this region (MRc2A2; MRc7F11; MRc10D6). (**B**) Results of the search for CpG islands using different approaches. (**C**) Putative exons and ORFs above 300 bp in the breakpoint region.

during development. An influence of chromosome rearrangement on the timing of transcription in certain developmental stages only would be compatible with the mild phenotype of the syndrome in our patient (26). Another developmental defect affecting forebrain and midface in a particular form of holoprosencephaly (*HPE3*) was shown to be caused by mutations affecting the sonic hedgehog (SHH) gene (32). In the *HPE3* example, translocations up to 230 kb 5′ to the gene have been implicated as the cause of the syndrome (33). As in our case, patients exhibiting deletions of the gene in question are generally more severely affected than the translocation patients (33). These observations support the hypothesis that proper development is dependent on exact levels of essential proteins such as *TWIST* and *SHH*. Any perturbations caused by environmental, or as in this case, genetic events could result in abnormal development.

The mechanism of the positional effect is still unresolved. In the patient described here, the breakpoint occurred 3′ to *TWIST* which is in contrast to the *SHH* example in *HPE3* where all of the breakpoints were 5′ to the gene. Other examples of putative positional effects in developmental disorders where the breakpoints were located 3′ to the gene include the *GLI3* gene in Greig acrocephalopolysyndactyly syndrome (34) and *PAX6* in aniridia (35). Although *TWIST* is the prime candidate for causing Saethre–Chotzen syndrome also in our case, we will still need to exclude the potential involvement of another gene(s) even closer to the translocation breakpoint. As suggested by the presence of a CpG island and putative exons near the breakpoint (Fig. 3) it is feasible that another gene or alternative forms of *TWIST* with etiology in Saethre–Chotzen syndrome might be identified. For example, we detected one cDNA clone which extended the published sequence 3′. The 3′ end of the genomic *TWIST* region contains several putative polyadenylation signals whose function, if any, will have to be evaluated.

The presence of genetic heterogeneity for Saethre–Chotzen syndrome has been suggested and at least one additional locus on 7p or elsewhere (20,23,36) in the genome might exist. The analysis of Saethre–Chotzen syndrome patients with chromosome 7 rearrangements as well as linkage studies in Saethre–Chotzen syndrome families indicate that other regions of 7p that do not include the immediate regions surrounding *TWIST* may be involved in the disease (20,23,36). Barring any influence from a *cis*-acting element or chromosome rearrangement far downstream of *TWIST*, it is entirely likely that another craniosynostosis gene may be found telomeric to the region described in this report. Therefore we have extended our transcriptional mapping experiments outwards from *TWIST* starting with the cosmid contig covering YAC 933_e_1.

Heterogeneity of the syndrome would fit well with observations in other craniosynostoses. Pfeiffer syndrome, for example,

is caused by mutations in different *FGFR* genes on chromosome 8cen (*FGFR1*) and 10q25–q26 (*FGFR2*) (8–10). When searching for candidates of additional Saethre–Chotzen syndrome loci, it is worth considering that in *Drosophila* the products of the zinc finger gene *Snail* and of *Twist* cooperate closely in the transcriptional regulation of *DFR1*, which is a *Drosophila* homolog to the human *FGFR* family. Also, Banfi and coworkers (37) mapped a region homologous to *Drosophila* Twist to human chromosome 2q37.3 in a region which might be paralogous to 7p. It will be interesting to see if *TWIST* has paralogous family members like *HOX*, *GLI* and *SP*, which are located in its neighbourhood on chromosome 7 (38).

MATERIALS AND METHODS

Patient

The clinical features of the male Japanese patient with some features of Saethre–Chotzen syndrome was previously described in detail (26). Briefly, the patient had CRS involving coronal and sagittal sutures and minor anomalies, scaphocephaly, narrow forehead, prominent eyes, mild upward slant of short and narrow palpebral fissures, long eyelashes, anteverted nares and apparently low-set and poorly lobulated ears. The patient had short 5th fingers but lacked the cutaneous syndactyly. Cytogenetic studies had revealed a *de novo* and apparently balanced translocation t(6;7)(q16.2;p15.3).

Library construction and cosmid contig formation

In order to construct a complete cosmid contig of the breakpoint region we subcloned the CEPH YAC 933_e_1 into SuperCos-1 vector (Stratagene). The cosmid library was prepared as described previously (39). Briefly, high molecular YAC DNA was isolated using sucrose gradient centrifugation according to Olson and coworkers (40). After purification, 10 µg DNA was digested with 0.5 and 0.05 U *Mbo*I, respectively, in a total volume of 100 µl. The fragment size of the individual fractions was tested in a 0.3% agarose gel. Fractions with an average size of 40–80 kb were pooled, dephosphorylated, precipitated and ligated into the *Bam*HI site of the cosmid vector SuperCos-1 (Stratagene). The ligation mix was then packed using the Gigapack II XL packing extract (Stratagene) and plated with *Escherichia coli* XL1-Blue MR (Stratagene). Human positive cosmid clones, which were identified by hybridization of colony filter lifts with human placental DNA, were gridded as duplicate spots onto Biodyne A membranes (Pall) using a Beckman Biomek 1000. These filters were screened with cosmid insert DNA and YAC insert end fragments (41) as probes. Positive clones were amplified and DNA was isolated according to standard procedures. Contigs were generated either by *Eco*RI restriction mapping or comparison of the *Alu* PCR banding pattern of individual clones after electrophoresis in 0.8% agarose gels. Cosmid DNA was blotted onto nylon membranes by alkaline transfer with 0.5 M NaOH and 1.5 M NaCl. To determine the cosmid *Eco*RI end fragments, T3 and T7 oligonucleotides were used as probes.

Fluorescence *in situ* hybridization (FISH)

The chromosomal localization of the t(6;7)(q16.2;p15.3) translocation breakpoint was carried out as described previously (43). In brief, biotin-7-dATP labelled total cosmid DNA from the individual cosmids of the tiling path was used as probe on metaphase spreads prepared from the patient's cell line.

cDNA preparation and selection

Randomly primed cDNA was prepared from poly(A)+ RNA of human fetal brain, fetal liver, placenta, adult liver tissue, and from the intestinal cell line CaCo-2 (ATCC HTB37). Selection was carried out for two consecutive rounds of hybridization to an immobilized pool of cosmid DNA from clones IIIB3, IIIA9, IIB11 and IID9, as described previously (43). Hybridizing cDNA was collected, passed over a G50 Fine Sephadex column, and amplified. The products were then digested with *Eco*RI, size selected on agarose gels, and ligated into pBluescript (Stratagene), that had been digested with *Eco*RI and treated with calf alkaline phosphatase (Boehringer Mannheim). Ligation products were transformed into competent DH5α *E.coli* cells (Life Technologies Inc.).

Characterization of retrieved cDNAs

For analysis of the cDNA clones individual colonies from the ligation were picked into microtiter plates, grown up and gridded onto Biodyne A membranes (PALL) to obtain colony hybridization filters. For the elimination of clones containing repetitive sequences, the filters were screened with cDNA made from total RNA. Plasmid DNA of the remaining clones was then prepared and used to produce probes for extensive characterization by hybridization of cosmid contig DNA filters and mammalian genomic DNAs. Clones which mapped back to the four cosmid clones and to chromosome 7, respectively, were analyzed by sequencing.

PCR amplification and sequencing of TWIST

Examination of the coding region of TWIST from the patient was carried out by using two primer pairs which were described previously (20,27). In brief, a 378 bp product representing the 5′-region was amplified using the forward primer 5′-GAG GCG CCC CGC TCT TCT CC-3′ and the reverse primer 5′-AGC TCC TCG TAA GAC TGC GGA C-3′ (20) and the 3′ portion of the coding region including a portion of the intron was amplified with the forward primer 5′-GCA AGC GCG GCA AGA AGT CT-3′ and the reverse primer 5′-GGG GTG CAG CGG CGC GGT C-3′ (27). The primer set amplifies a 461 bp product. The PCR products were run on a 1.2% agarose gel, excised from the gel and the DNA isolated with a Gel Extraction Kit (Quiagen). Isolated PCR product was sequenced in both directions on a model 373 automated DNA sequencer (Applied Biosystems).

Probe generation and Southern blotting

Methods employed for the isolation of high-molecular-weight DNA, restriction-endonuclease digestion, as well as separation and blotting of DNA fragments have been described elsewhere (44).

Genomic DNA from the patient and the control cell lines was digested by several restriction enzymes. Identical amounts (10 µg) were loaded on a 0.8% agarose gel and transferred onto a nylon membrane (Biodyne A membranes, Pall). Probes A, B and C are PCR products using STS primers described in Table 1. Random primed labelling with [α-^{32}P]dCTP was performed according to standard procedures. Hybridization of genomic blots

and cDNA colony hybridization filters was performed overnight at 60°C using the hybridization mix described by Church and Gilbert (45). Membranes were washed with the final stringency of 0.2× SSC and 0.1% SDS at 60°C.

Sequencing and sequence analysis

For primer walk sequencing, specific restriction fragments were subcloned and used as template. Sequence reactions with cDNA clones and genomic subclones were performed using an ABI PRISM Dye terminator cycle sequencing ready reaction kit (Perkin Elmer) and vector specific or sequence derived primers. Sequence assembly was performed by the software package Sequencher (Gene Codes, Ann Arbor). Nucleic and amino acid searches of DNA, protein and EST databases were performed by the software BCM Search-Launcher:

(http://gc.bcm.tmc. edu:8088/search-launcher/launcher.html).

Searches for sequence homologies were made with the BLAST program (46), for potential exon structures and CpG islands with GRAIL (47), and for repeat sequence with PYTHIA (48).

Molecular analysis of the derivative chromosome $7p^+$ and $6q^-$ translocation fragment

Cloning and characterization of the 2.7 kb *Eco*RI der(7) and the 3.7 kb *Pst*I der(6) breakpoint fragment was performed as described by Toriello and coworkers (49) with slight modifications. In brief, 10 µg of the patient's genomic DNA was digested by *Eco*RI and *Pst*I, respectively, and size selected on a 1% agarose gel. The 2.7 kb *Eco*RI and the 3.7 kb *Pst*I DNA fractions containing the rearranged fragments were purified (QiaexII kit) and ligated into *Eco*RI or *Pst*I digested, dephosphorylated pBluescript II KS(+) (Stratagene). *Eco*RI ligation products were amplified using vector specific primers M13 and Rev in a 50 µl reaction. To obtain the der(7) breakpoint sequences M13/Rev PCR products were used as template, a second round of PCR was performed with the chromosome 7 insert specific primer MR22004 (5′-GTT TAT CTT GCC CAG ATG TTA GGG-3′) and a pBluescript specific primer (5′-GGA AAC AGC TAT GAC CAT GAT TAC-3′). Then, a third, nested PCR was performed using chromosome 7 specific nested primer MR22003 (5′-AGG GCT TTT ATG AAA TGT CAC GTG-3′) and pBluescript specific nested primer 5′-GCGCATTAACCCT-CACTAAAGGG-3′ (both rounds of insert specific PCR were performed with the annealing temperature of 62°C). These conditions produced a specific product from the 2.7 kb fraction of ~1.8 kb length. The last two rounds of PCR employed long-distance PCR conditions using the Expand Long Range PCR System (Boehringer Mannheim) following the manufacturer's instructions. The resulting 1.8 kb PCR product was sequenced directly after gel purification by primer walking. To obtain the der(6) breakpoint sequences, nested PCR from *Pst*I-ligation products as template were performed using pBluescript specific primers as described above and a chromosome 7 specific primer MR22010 (5′-ATTATGCCTGT-AGGAAGCC-3′). Both rounds of PCR required an annealing temperature of 55°C. The resulting PCR product of ~600 bp length representing the breakpoint from the telomeric side was sequenced directly after gel purification. In both cases, successive rounds of PCR employed 1.0 µl of product from the previous round of PCR as template.

Cell lines and cell hybrids

The hybrid cell line 5387-3cl10 containing chromosome 7 as the only human material was a gift from Dr C. Croce (50). GM3104 was obtained from the NIGMS Human Genetic Mutant Cell Repository.

ACKNOWLEDGEMENTS

The skilful technical assistance of D. Bornholdt and H. Engel is gratefully acknowledged. The authors thank A. Schelbert and Dr B. Horsthemke for helpful discussions, and Dr J. Evans for the Chinese hamster cell line RJK. This work was supported by grants from the Deutsche Forschungsgemeinschaft (DFG: Ku1001/2-2) and the Stiftung P.E. Kempkes (Marburg, Germany).

REFERENCES

1. Heutink, P., Vermeeij-Keers, C. and Oostra, B.A. (1995) The genetic background of craniosynostosis syndromes. *Eur. J. Genet.* **3**, 312–323.
2. Lammer, E.J., Cordero, J.F., Wilson, M.J., Oimette, D. and Ferguson, S. (1987) Investigation of a suspected increased prevalence of craniosynostosis: Colorado, 1978–1982. *Proc. Greenwood Genet. Cent.* **6**, 126–127.
3. Winter, R.M. and Baraitser, M. (1994) The London Dysmorphology database. Oxford, Oxford University Press
4. Cohen, M.M. Jr. (1986) *Craniosynostosis: Diagnosis, Evaluation, and Management.* Raven Press, New York.
5. Blank, C.E. (1960) Apert's syndrome (a type of acrocephalosyndactyly): Observations on a British series of thirty-nine cases. *Ann. Hum. Genet.* **24**, 151–164.
6. Wilkie, A.O.M., Slaney, S.F., Oldridge, M., Poole, M.D., Ashworth, G.J., Hockley, A.D., Hayward, R.D., David, D.J., Pulleyn, L.J., Rutland, P., Malcolm, S., Winter, R.M. and Reardon, W. (1995) Apert syndrome results from localized mutations of *FGFR2* and is allelic with Crouzon syndrome. *Nature Genet.* **9**, 165–172.
7. Jabs, E. W., Li, X., Scott, A. F., Meyers, G., Chen, W., Eccles, M., Mao, J. I., Charnas, L. R., Jackson , C. E. and Jaye, M. (1994). Jackson–Weiss and Crouzon syndromes are allelic with mutations in fibroblast growth factor receptor 2. *Nature Genet.* **8**, 275–279.
8. Lajeunie, E., Ma, H.W., Bonaventure, J., Munnich, A., Le Merrer, M. and Renier, D. (1995) *FGFR2* mutations in Pfeiffer syndrome. *Nature Genet.* **9**, 108.
9. Rutland, P., Pulleyn, L.J., Reardon, W., Baraitser, M., Hayward, R.D., Jones, B., Malcolm, S., Winter, R.M., Oldridge, M., Slaney, S.F., Poole, M.D. and Wilkie, A.O.M. (1995) Identical mutations in the *FGFR2* gene cause both Pfeiffer and Crouzon syndrome phenotypes. *Nature Genet.* **9**, 173–176.
10. Schell, U., Hehr, A., Feldman, G.J., Robin, N.H., Zackai, E.H., de Die-Smulders, C., Viskochil, D.H., Stewart, J.M., Wolff, G., Hirofumi, O., Price, A.R., Cohen, M.M., and Muenke, M. (1995) Mutations in *FGFR1* and *FGFR2* cause familial and sporadic Pfeiffer syndrome. *Hum. Mol. Genet.* **4**, 323–328.
11. Reardon, W., Winter, R.M., Rutland, P., Pulleyn, L.J., Jones, B.M. and Malcolm, S. (1994). Mutations in the fibroblast growth factor receptor 2 gene causes Crouzon syndrome. *Nature Genet.* **8**, 98–103
12. Gorry, M.C., Preston, R.A., White, G.J., Zhang, Y., Singhai, V.K., Losken, H.W., Parker, M.G., Nwokoro, N.A., Post, J.C. and Ehrlich, G.D. (1995) Crouzon syndrome: mutations in two spliceforms of *FGFR2* and a common point mutation shared with Jackson–Weiss syndrome. *Hum. Mol. Genet.* **5**, 1387–1390.
13. Ma, H.W., Lajeunie, E., Le Merrer, M., de Parseval, N., Serville, F., Weissenbach, J., Munnich, A. and Renier, D. (1995) No evidence of genetic heterogeneity in Crouzon craniofacial dysostosis. *Hum. Genet.* **96**, 731–735.

14. Oldridge, M., Wilkie, A.O.M., Slaney, S.F., Poole, M.D., Pulleyn, L.J., Rutland, P., Hockley, A.D., Wake, M.J.C., Goldin, J.H., Winter, R.M., Reardon, W. and Malcom, S. (1995) Mutations in the third immunoglobulin domain of the fibroblast growth factor receptor-2 gene in Crouzon syndrome. *Hum. Mol. Genet.* **4**, 1077–1082.
15. Park, W.- J., Meyers, G.A., Li, X., Theda, C., Day, D., Orlow, S.J., Jones, M.C. and Jabs, E.W. (1995) Novel *FGFR2* mutations in Crouzon and Jackson–Weiss syndromes show allelic heterogeneity and phenotypic variability. *Hum. Mol. Genet.* **4**, 1229–1233.
16. Steinberger, D., Mulliken, J.B. and Müller, U. (1995) Predisposition for cystein substitution in the immunoglobulin-like chain of *FGFR2* in Crouzon syndrome. *Hum. Genet.* **96**, 113–115.
17. Slaney, S.F., Oldridge, M., Hurst, J.A., Morris-Kay, G.M., Hall, C.M., Poole, M.D. and Wilkie, A.O.M. (1996) Differential effects of *FGFR2* mutations on syndactyly and cleft palate in Apert syndrome. *Am. J. Hum. Genet.* **58**, 923–932.
18. Saethre, M. (1931) Ein Beitrag zum Turmschädelproblem (Pathogenese, Erblichkeit und Symptomatologie). *Dtsch Z. Nervenheikd.* **119**, 533–555
19. Chotzen, F. (1932) Eine eigenartige familiäre Entwicklungsstörung (Akrocephalosyndaktylie, Dystosis craniofacialis und Hypertelorismus).*Monatsschr. Kinderheilkd.* **55**, 97–122.
20. Howard, T.D., Paznekas, W.A., Green, E., Chiang, L.C., Ma, N., Isela, R., De Luna, O., Delgado, C.G., Gonzales-Ramos, M., Kline, A.D. and Jabs, E.W. (1997) Mutations in *TWIST*, a basic helix–loop–helix transcription factor, in Saethre–Chotzen syndrome. *Nature Genet.* **15**, 36–41
21. Brueton ,L.A., Herwerden ,L. van, Chotai, K.A. and Winter, R.M. (1992) Mapping of a gene for craniosynostosis: evidence for linkage of Saethre–Chotzen syndrome to distal chromosome 7p. *J. Med. Genet.* **29**, 681–685.
22. Lewanda, A.F., Cohen, M.M., Jackson, C.E., Taylor, E.W., Li, X., Beloff, M., Day, D., Clarren, S.K., Ortiz, R., Garcia, C., Hauselman, E., Figueroa, A., Wulfsberg, E., Wilson, M., Warman, M.L., Padwa, B.L., Whiteman, D.A.H., Mulliken, J.B. and Jabs, E.W. (1994) Genetic heterogeneity among craniosynostosis syndromes: Mapping the Saethre–Chotzen syndrome locus between D7S513 and D7S516 and exclusion of Jackson–Weiss and Crouzon syndrome loci from 7p. *Genomics* **19**, 115–119.
23. Lewanda, A.F., Green, E.D., Weissenbach, J., Jerald, H., Taylor, E., Summar, M.L., Phillips, J.A., Cohen, M., Feingold, M., Mouradian, W., Clarren, S.K. and Jabs, E.W. (1994) Evidence that the Saethre–Chotzen syndrome locus lies between D7S664 and D7S507, by genetic analysis and detection of a microdeletion in a patient. *Am. J. Hum. Genet.* **55**, 1195–1201
24. Rose, C. S., King, A. A., Summers, D., Palmer, R., Yang, S., Wilkie, A. O., Reardon, W., Malcolm, S. and Winter, R. M. (1994) Localization of the genetic locus for Saethre–Chotzen syndrome to a 6 cM region of chromosome 7 using four cases with apparently balanced translocations at 7p21.2. *Hum. Mol. Genet.* **3**, 1405–1408.
25. van Herwerden, L., Rose, C.S., Reardon, W., Brueton, L.A., Weissenbach, J., Malcolm, S. and Winter, R.M. (1994) Evidence for locus heterogeneity in acrocephalosyndactyly: A refined localization for the Saethre–Chotzen syndrome locus on distal chromosome 7 and exclusion of Jackson–Weiss syndrome from craniosynostosis loci 7p and 5q. *Am. J. Hum. Genet.* **54**, 669–674.
26. Tsuji,K., Narahara,K.,Kikkawa, M., Murakami, Y., Yokoyama,Y., Ninomiya, S. and Seino, Y. (1994) Craniosynostosis and hemizygosity for D7S135 caused by a de novo and apparently balanced t(6;7) translocation.*Am. J. Med. Genet.* **49**, 98–102.
27. El Ghouzzi, V., Merrer, M.L., Perrin-Schmitt, F., Lajeunie, E., Benit, P., Renier, D., Bourgeois, P., Bolcato-Bellemin, A.-L., Munnich, A. and Bonaventure, J. (1997) Mutations of the *TWIST* gene in Saethre–Chotzen syndrome. *Nature Genet.* **15**, 42–46
28. Tsuji, K., Narahara, K., Yokoyama, Y., Grzeschik, K.-H. and Kunz, J. (1995) The breakpoint on 7p in a patient with t(6;7) and craniosynostosis is spanned by a YAC clone containing the D7S503 locus. *Hum. Genet.* **95**, 303–307.
29. Bernardi, G. (1993) The isochore organization of the human genome and its evolutionary history-A review. *Gene* **135**, 57–66.
30. Chen, Z.-F., and Behringer, R.R. (1995) Twist is required in head mesenchyme for cranial neural tube morphogenesis. *Genes Dev.* **9**, 686–699.
31. Felsenfeld, G. (1996) Chromatin unfolds. *Cell* **86**, 13–19.
32. Roessler, E., Belloni, E., Gaudenz, K., Jay, P., Berta, P., Scherer, S.W., Tsui, L.-C., and Muenke, M. (1996) Mutations in the human *sonic hedgehog* gene cause holoprosencephaly. *Nature Genet.* **14**, 357–360.
33. Belloni, E., Muenke, M., Roessler, E., Traverso, G., Siegel-Bartelt, J., Frumkin, A., Mitchell, H.F., Donis-Keller, H., Helms, C., Hing, A.V., Heng, H.Q.H., Koop, B., Martindale, D., Rommens, J.M., Tsui, L.-C., and Scherer, S.W. (1996) Identification of *sonic hedgehog* as a candidate gene responsible for holoprosencephaly. *Nature Genet.* **14**, 353–356.
34. Vortkamp, A., Gessler, M. and Grzeschik, K.- H. (1991) GLI3 zinc-finger gene interrupted by translocations in Greig syndrome families. *Nature* **352**, 539–540.
35. Fantes, J., Redeker, B., Breen, M., Boyle, S., Brown, J., Fletcher, J., Jones, S., Bickmore, W., Fukushima ,Y., Mannens, M., Danes, S. and van Heyningen, V. (1995) Aniridia-associated cytogenetic rearrangements suggests that a position effect may cause the mutant phenotype. *Hum. Mol. Genet.* **4**, 415–422.
36. von Gernet, S., Schuffenhauer, S., Golla, A., Lichtner, P., Balg, S., Mühlbauer, W., Murken, J., Fairly, J., and Meitinger, T. (1996) Craniosynostosis suggestive of Saethre–Chotzen syndrome: Clinical description of a large kindred and exclusion of candidate regions on 7p. *Am. J. Med. Genet.* **63**, 177–184.
37. Banfi, S., Borsani, G., Rossi, E., Bernard, L., Guffanti, A., Rubboli, F., Marchitiello, A., Giglio, S., Coluccia, E., Zollo, M., Zuffardi, O. and Ballabio, A. (1996) Identification and mapping of human cDNAs homologous to *Drosophila* mutant genes through EST database searching. *Nature Genet.* **13**, 167–174.
38. Tsui, L.-C., Donis-Keller, H. and Grzeschik, K.-H. (1995). Report of the second international workshop on human chromosome 7 mapping 1994. *Cytogenet. Cell Genet.* **71**, 2–21.
39. Vortkamp, A., Gessler, M., Le Paslier, D., Elaswarapu, R., Smith, S. and Grzeschik, K.-H. (1994) Isolation of a yeast artificial chromosome contig spanning the Greig cephalopolysyndactyly syndrome (GCPS) gene region. *Genomics* **22**, 563–568.
40. Olson, M.V., Loughney, K. and Hall, B. D. (1979) Identification of the yeast DNA sequences that correspond to specific tyrosine-inserting nonsense suppressor loci. *J. Mol. Biol.* **132**, 387–410
41. Kere, J., Nagaraja, R., Mumm, S., Ciccodicola, A., D'Urso, M. and Schlessinger, D. (1992) Mapping human chromosomes by walking with sequence-tagged sites from end fragments of yeast artificial chromosome inserts. *Genomics* **14**, 241–248.
42. Kunz, J., Scherer, S.W. , Klawitz, I., Soder, S., Du, Y.-Z., Speich, N., Kalff-Suske, M., Heng, H. H.Q., Tsui, L.-C., and Grzeschik, K.-H. (1994) Regional localization of 725 human chromosome 7-specific yeast artificial chromosome (YAC) clones. *Genomics* **22**, 439–448.
43. Rommens, J.M., Mar, L., McArthur, J, Tsui, L.-C. and Scherer, S.W. (1994) In Hochschwender, and Gardiner, K. (eds) *The Identification of Transcribed Sequences*, Plenum Press, pp. 65–79.
44. Sambrook, J., Fritsch, E.F. and Maniatis, T (1989) *Molecular Cloning: A Laboratory Manual.* Cold Spring Harbour Laboratory Press, Cold Spring Harbour, NY.
45. Church, G.M., and Gilbert, W. (1984). Genomic sequencing. *Proc. Natl. Acad. Sci. USA* **81**, 1991–1995.
46. Altschul, S.F., Gish, W., Miller, W. and Lipman, D.J. (1990) Basic local alignment search tool. *J. Mol. Biol.* **215**, 403–410.
47. Uberbacher, E. C. and Mural, R. J. (1991) Locating protein-coding regions in human DNA sequences by a multiple sensor-neural network approach. *Proc. Natl. Acad. Sci. USA* **88**, 11261–11265.
48. Zuo, J., Robbin, C., Taillon-Miller, P., Cox, D.R. and Myers, R.M. (1992) Cloning of the Huntington disease region in yeast artificial chromosomes. *Hum. Mol. Genet.* **1**, 149–159.
49. Toriello, H.V., Glover, T.W., Takahara, K., Byers, P.H., Miller, D.E., Higgins, J.V. and Greenspan, D.S. (1996) A translocation interrupts the COL5A1 gene in a patient with Ehlers–Danlos syndrome and hypomelanosis of Ito. *Nature Genet.* **13**, 361–365.
50. Croce, C.M. and Koprowski, H. (1974) Somatic cell hybrids between mouse peritoneal macrophages and SV40 transformed human cells. I. Positive control of the transformed phenotype by the human chromosome 7 carrying the SV40 genome. *J. Exp. Med.* **139**, 1350–1353.